

Mass dose effects and in vivo affinity in brain PET receptor studies — a study of cerebral 5-HT₄ receptor binding with [¹¹C]SB207145[☆]

Karine Madsen^{a,*}, Lisbeth Marner^a, Mette Haahr^a, Nic Gillings^b, Gitte M. Knudsen^a

^aNeurobiology Research Unit, The Neuroscience Center, Rigshospitalet, DK-2100 Copenhagen, Denmark

^bPET and Cyclotron Unit, Rigshospitalet, DK-2100 Copenhagen, Denmark

Received 12 January 2011; received in revised form 28 February 2011; accepted 28 April 2011

Abstract

Attention to tracer dose principles is crucial in positron emission tomography (PET), and deviations can induce serious errors. In this study, we devise a method for determining receptor occupancy of the mass dose of the radioligand itself and the in vivo affinity.

Methods: The approach was used for [¹¹C]SB207145, a new PET radioligand for imaging the cerebral 5-HT₄ receptors in humans. Test–retest PET studies with varying specific activities of [¹¹C]SB207145 were conducted in seven healthy subjects, and the output parameter regional BP_{ND} was modeled. Individual occupancy plots were first computed to estimate the mass dose that saturates 50% of receptors (ID_{50}), and subsequently, the maximal mass dose that can be injected (arbitrarily set at an occupancy <5%) was calculated. Scatchard plots were computed to estimate the in vivo K_D .

Results: Increasing the mass dose resulted in a decrease in BP_{ND} , whilst the relative cerebellar uptake was unchanged. The ID_{50} was 85.4 ± 30.2 μ g, and the upper mass dose limit was 4.5 ± 1.6 μ g, which does not require ultrahigh specific activity. The estimated in vivo K_D was 2.8 nM (range 1.0–4.8), without any regional differences.

Conclusion: The presented method for estimating the upper mass dose limit is suggested as part of validation of PET radioligands.

© 2011 Elsevier Inc. All rights reserved.

Keywords: PET; Injected mass; Mass dose; Occupancy; K_D ; Human

1. Introduction

Methods for the production of radioligands for positron emission tomography (PET) are continuously improving, and over the years, efforts have been made to improve the specific activity, such that injection of a chemical amount of a ligand (mass dose) of a few micrograms or less can be achieved. A low mass is in keeping with tracer principles and may also sometimes be needed to avoid pharmacological or potentially toxic effects. Reliable quantitative estimates of binding potentials (BP) require negligible ligand occupancy of the target receptors/transporters, often

referred to as <5% to 10% [1]. Thus, investigation of mass dose effects should be considered a mandatory part of a thorough PET radioligand validation. We here present a method for estimating the mass dose of a ligand that saturates 50% of receptors (ID_{50}) from which the mass dose limits can be calculated. The method involves test–retest studies for the construction of individual occupancy plots (a modification of which is also termed the “Lassen Plot”) [2,3], but neither true “zero occupancy” scans nor very high occupancy scans are required.

Radioligands that may be particularly prone to exhibit pharmacological or occupancy effects include agonist radiotracers or compounds with a high plasma free fraction or slow metabolic rate (\uparrow brain uptake), a high transfer from the plasma to tissue (\uparrow K_1) or a high receptor affinity (low K_D). For example, high specific activity is needed with the high-affinity D₂/D₃ receptor agonist [¹¹C](+)-PHNO because pharmacological effects are seen at mass doses above 3 μ g [4], and the upper mass dose limit for human studies

[☆] Disclosures: All authors report no actual or potential financial or personal conflicts of interest.

* Corresponding author. Neurobiology Research Unit N9201, University Hospital Rigshospitalet, Blegdamsvej 9, DK-2100 Copenhagen O, Denmark. Tel.: +45 3545 6708; fax: +45 3545 6708.

E-mail address: karine@nru.dk (K. Madsen).

with [^{11}C](+)-PHNO has been estimated to be 0.5 μg (<10% occupancy) [5]. Likewise, the high-affinity H_3 receptor antagonist [^{11}C]GSK189254 has an upper mass dose limit of around 0.2 μg (<5% occupancy) [6], and the upper mass dose limit of the high-affinity D_2 receptor [^{11}C]FLB 457 is 0.5 μg [7]. The occupancy of the mass dose and the upper mass dose limit can be estimated from population-based studies [8] or from estimations of the oral dose of ligand that occupies 50% of available receptor sites (ED_{50}) [6]. Alternatively, the occupancy can be estimated by dividing the concentration of receptor-bound ligand in tissue with the density of receptors (B_{max}) in the same region, which can be measured either from Scatchard plots of test–retest studies [7] or from autoradiography studies.

[^{11}C]SB207145 is currently the only PET radioligand available for imaging the 5-HT $_4$ receptor in vivo in the central nervous system of humans, and since experimental studies have suggested the 5-HT $_4$ receptor to be involved in cognitive function [9], depression [10] and Alzheimer's disease [11,12], in vivo investigations of the 5-HT $_4$ receptor in humans are highly interesting. We know that [^{11}C]SB207145 crosses the blood–brain barrier fairly well and that it is a 5-HT $_4$ receptor antagonist with suitable kinetics for quantification of the 5-HT $_4$ receptor [13]. Although [^{11}C]SB207145 has high affinity to the 5-HT $_4$ receptor, it binds reversibly within the time window of a 2-h dynamic PET scan. It has a relatively slow metabolic rate and high free fraction in plasma (around 27%). We have previously made a population-based estimate of the upper limit of mass dose of 1.2 μg (occupancy <5%), which requires a fairly high specific activity [8]. Further, [^{11}C]SB207145 binding has been shown to be unaffected by acute increase of endogenous serotonin [8].

The aim of this study was to investigate the ligand mass dose effects on receptor occupancy, radioligand metabolism and free fraction in plasma. The mass dose required to saturate 50% of receptors (ID_{50}) and the upper limit for mass dose of [^{11}C]SB207145 for both maximum 5% (D_5) and 10% (D_{10}) occupancy are estimated from test–retest studies with varying mass dose in a test–retest design. Finally, the in vivo concentration of free ligand in tissue required to saturate 50% of receptors (in vivo K_D) is calculated from the test–retest studies with larger differences in mass dose.

2. Methods

2.1. Subjects

Seven subjects were included in the study (five men and two women, mean age 40 years, range 20–57, mean body weight 81 kg, range 63–98). The subjects gave a written informed consent for participation, and the study was approved by The Copenhagen Region Ethics Committee [(KF)01-274821 and (KF)01 2006-2, with amendments]. Exclusion criteria were significant medical history, drug or alcohol abuse, neurological or psychiatric disorders, men-

tally deficiency (ensured with DART45, which is a Danish version of the National Adult Reading Test [14]), pregnancy or head trauma. All subjects had a normal neurological examination and unremarkable brain magnetic resonance imaging (MRI) scans. Absence of significant psychiatric symptoms was ensured using the Symptom Check List Revised [15] on the day of the PET scans.

2.2. MRI and regions of interest

Magnetic resonance imaging was conducted on a Siemens Magnetom Trio 3-T MR scanner (matrix 256×256; 1×1×1-mm voxels). The T1-weighted MRIs were segmented into grey matter, white matter and cerebrospinal fluid using Statistical Parametric Mapping (SPM5; Wellcome Department of Cognitive Neurology, London, UK). The T2-weighted images served for brain masking purposes. Twenty regions were automatically delineated on each subject's MRI in a user-independent fashion with the Pvelab software package [16] (freely available on www.nru.dk/downloads); the mean grey matter volumes of the regions are given in parentheses:

- Striatal regions (high 5-HT $_4$ receptor binding): caudate nucleus (4.2 ml) and putamen (6.7 ml).
- Limbic regions (intermediate 5-HT $_4$ receptor binding): hippocampus (5.8 ml), entorhinal cortex (3.5 ml), amygdala (2.0 ml), anterior cingulate gyrus (6.6 ml), posterior cingulate gyrus (4.7 ml) and thalamus (8.5 ml).
- Neocortical regions (low 5-HT $_4$ receptor binding): orbitofrontal cortex (18.8 ml), medial and inferior frontal gyri (57.2 ml), superior frontal gyrus (43.4 ml), insula (14.9 ml), superior temporal gyrus (37.3 ml), medial and inferior temporal gyri (43.6 ml), sensory motor cortex (40.0 ml), parietal cortex (60.2 ml), occipital cortex (54.6 ml), dorsolateral prefrontal cortex (17.9 ml) and ventrolateral prefrontal cortex (12.0 ml).
- Reference region (negligible concentration of 5-HT $_4$ receptors): cerebellum, excluding vermis (79 ml).

2.3. PET scanning

The PET scans were performed with an 18-ring GE-Advance scanner (General Electric, Milwaukee, WI, USA) operating in 3D acquisition mode and producing 35 image slices with an interslice distance of 4.25 mm. The total axial field of view was 15.2 cm, with an approximate in-plane resolution of 6 mm. To minimize movement during the scan, a light headband fixation was used. The scan was based on a 120 min dynamic acquisition starting with a bolus injection of mean 542 MBq (range 366–604 MBq) [^{11}C]SB207145 given over 20 s. The acquisition consisted of 38 time frames, increasing progressively in duration from 5 s to 10 min.

After acquisition, attenuation and decay-corrected recordings were reconstructed by filtered back projection using a 6-mm Hann filter. Frames were aligned using AIR 5.2.5

Table 1

Individual mass doses normalized to 70 kg of body weight and the corresponding estimates of ID_{50} , D_{10} and D_5 based on graphical analysis of occupancy plots (see example in Fig. 1B)

	Mass dose (μg)		Occupancy plots		Mass dose limits (μg)		
	D_{Low}	D_{High}	α	R^2	ID_{50}	D_5	D_{10}
Subject 1	4.9	21.9	0.85	0.99	94.3	5.0	10.5
Subject 2	4.2	17.0	0.80	0.97	50.2	2.6	5.6
Subject 3	3.7	15.6	0.91	0.99	110.7	5.8	12.3
Subject 4	0.3	4.4	0.93	0.99	53.6	2.8	6.0
Subject 5	0.7	4.1	0.95	1.00	66.9	3.5	7.4
Subject 6	2.4	4.3	0.98	0.99	93.7	4.9	10.4
Subject 7	2.7	4.2	0.99	0.99	131.1	6.9	14.6
Mean \pm S.D.	2.7 \pm 1.7	10.2 \pm 7.7	0.92 \pm 0.07		85.8 \pm 30.2	4.5 \pm 1.6	9.5 \pm 3.3

The slope α is the ratio between the high- and low-dose studies; R^2 designates the correlation coefficient. The mass doses giving 50% occupancy, ID_{50} , are listed together with the upper mass dose limits (occupancy <5% and <10%).

[17] to correct for movements during the scan. Before alignment, each frame was filtered with a 12-mm Gaussian filter, and the rigid transformation was estimated for each frame to a selected single frame with sufficient structural information (frame 26: 15–20 min postinjection). The [^{11}C] SB207145 PET scans were automatically co-registered to the MRI with the AIR algorithm [17] using only the mean of the first 20 min of the PET scan corresponding to a flow-weighted image. The quality of each co-registration was evaluated by visual inspection in three planes. Regional time activity curves (TACs) were constructed from grey matter voxels in VOIs, and kinetic modeling was performed with the simplified reference tissue model (SRTM) using cerebellum as reference region as previously validated [13]. The regional in vivo outcome measure for 5-HT $_4$ receptor density is the binding potential, BP_{ND} , relative to the nondisplaceable binding of the radioligand (including both nonspecific binding and the free radioligand) represented by the cerebellum. The kinetic modeling was performed using the PMOD software version 2.9, build 2 (PMOD Technologies).

Test–retest studies were conducted in all subjects in random order: one scan was performed with a high specific activity and low mass dose (D_{low}) of unlabelled ligand, and one scan was performed with low specific activity and high mass dose (D_{high}) (Table 1). In three subjects, the mass dose difference was >10 μg ; in two subjects, it was 3–5 μg ; and in two subjects, it was 1–2 μg . All mass doses were normalized to 70 kg of body weight. Three of the test–retest studies were conducted with the high mass dose first and four with the low mass dose first. To avoid mass carryover effects, the time interval between the first and the second scan was >3 weeks, except in the two subjects with small mass dose differences (subjects 6 and 7) where studies were carried out the same day. No clinical side effects were observed after [^{11}C] SB207145 injection.

Immediately before radiotracer injection, venous blood samples were drawn and used to measure the plasma free fraction, f_p , with equilibrium dialysis as described previously [18].

Venous blood samples were also drawn 55 min after injection, and fraction of parent [^{11}C]SB207145 and its radiolabelled metabolites in plasma were measured with high-performance liquid chromatography, as previously described [19].

2.4. Data analysis

At equilibrium conditions, the concentration of receptor bound ligand (B) is determined by the Michaelis–Menten equation

$$B = \frac{B_{\text{Max}}F}{K_D + F} \quad (1)$$

where B_{max} is the density of receptors, F is the concentration of free radioligand and K_D is the dissociation constant. At low dose, mass of radioligand is $F \ll K_D$ and Eq. (1) reduces to

$$\frac{B}{F} = \frac{B_{\text{Max}}}{K_D} = BP \quad (2)$$

The outcome of SRTM is the nondisplaceable binding potential, BP_{ND} , which is proportional (by the free tissue fraction, f_{ND}) to, but does not equal, B_{max}/K_D .

Under the assumption that full occupancy of receptor sites would be approached at high mass dose, the receptor occupancy (O) will be determined by the mass dose (D) and ID_{50} of the ligand

$$O = \frac{D}{D + ID_{50}} \quad (3)$$

Under the further assumption that the underestimated BP by mass dose (BP_{Occupied}) is given by the nonoccupied BP (BP_{Baseline}) and O by the equation

$$BP_{\text{Occupied}} = (1 - O)BP_{\text{Baseline}} \quad (4)$$

then the ID_{50} can be estimated from the test–retest studies with varying mass doses, by individual occupancy plots: The

19 regional BP_{ND} s of the scan using a high mass dose are plotted against the corresponding regional BP_{ND} of the scan using a low mass dose. The occupancy plots needs no true “zero occupancy” (baseline) scan, like in the “Lassen Plot revisited” [3], and the occupancy plots are here based on BPs rather than distribution volumes. The individual ID_{50} can then be calculated by using the slope (α) of the regression line in the occupancy plot, where $\alpha < 1$ represents the negative effect of higher mass dose on BP_{ND}

$$\alpha = \frac{1 - O_{High}}{1 - O_{Low}} = \frac{1 - \frac{D_{High}}{D_{High} + ID_{50}}}{1 - \frac{D_{Low}}{D_{Low} + ID_{50}}} \quad (5)$$

$$= \frac{D_{Low} + ID_{50}}{D_{High} + ID_{50}} \Leftrightarrow$$

$$ID_{50} = \frac{\alpha D_{High} - D_{Low}}{1 - \alpha}$$

The ID_{50} was calculated for each of the seven subjects. The corresponding upper mass dose limits, D_5 and D_{10} , are then calculated by rearranging Eq. (3).

The fraction of parent compound in plasma 55 min postinjection was compared between scans with high mass dose and low mass dose, using the Wilcoxon two-sample test ($N=7$), to measure the effect of mass dose on radioligand metabolic rate. The effect of mass dose on the free fraction of ligand in plasma ($N=5$) was analyzed similarly. In addition, we compared the concentration of free parent compound in plasma with the cerebellar concentration and calculated the ratio between free and nonspecific binding ($N=9$) under the assumption that, 55 min postinjection, the free fraction in plasma equals that of cerebellum.

The in vivo concentration of free ligand in tissue required to saturate 50% of receptors, the dissociation constant K_D , was estimated individually using Scatchard plots: The slope equals $-1/K_D$ when regional BP_{ND} is plotted against the concentration of receptor-bound ligand in the tissue of the same region. To minimize noise, the individual K_D was estimated only from volume-weighted averages of the high-binding region striatum and the global neocortex and only in subjects where the difference in mass dose in test–retest scans was above 3 μg ($N=5$). The concentration of receptor-bound ligand in a region was measured as the mean ligand concentration in the region 80–120 min postinjection subtracted by the mean cerebellar concentration (representing free and nonspecific bound ligand only). The time interval was chosen so that the cerebellar concentration was relatively stable (mean $15\% \pm 2\%$ decrease during the interval 80–120 min postinjection). An example of a time concentration curve is given in Fig. 1A.

3. Results

Table 1 shows the individual mass doses and the estimated values of ID_{50} , D_{10} and D_5 . Occupancy plots were performed

for each test–retest study (see example in Fig. 1B). Increasing the mass dose reduced BP_{ND} in all test–retest studies (see slope < 1 in Table 1), whilst the cerebellar area under the curve TAC (AUC) normalized to the mean injected activity (542 MBq) was unchanged ($P=.75$, paired t test). Based on the individually measured mass dose effects, an average ID_{50} of $85.4 \pm 30.2 \mu\text{g}$ was found [Eq. (5)]. Despite test–retest variability, ID_{50} does not seem to vary more in subjects studied with low dose differences, and the association between mass dose and occupancy, described by Eq. (3), is illustrated in Fig. 2. This corresponds to 5% receptor occupancy at a mass dose of $4.5 \pm 1.6 \mu\text{g}$ and 10% receptor occupancy at $9.5 \pm 3.3 \mu\text{g}$.

The mean fraction of parent compound in plasma 55 min postinjection was similar ($P=.70$) in scans with low and with high mass dose: $10\% \pm 2\%$ and $10\% \pm 3\%$, respectively. Similarly, f_p was similar ($P=.37$) in scans with low and with high mass dose: $29\% \pm 7\%$ and $25\% \pm 4\%$, respectively. Fifty-five minutes postinjection, the concentration of free parent compound in plasma was mean 5 pM (range 0.1–17 pM), and the cerebellar concentration was mean 420 pM (range 11–1205 pM) 55 min postinjection. Under the rigid assumption of equilibrium conditions at this time point, the free accounted for only $1.5\% \pm 0.6\%$ of the nondisplaceable binding in cerebellum.

The individual graphically estimated average K_D was 3.3 nM (range 2.2–4.8) in the striatum and 2.4 nM (1.0–4.4) in the neocortex (Fig. 3). There was no significant difference in K_D between these regions ($P=.16$, paired t test).

4. Discussion

The study provides a new simple method for investigating the effects of mass dose in brain PET receptor studies. This is exemplified with the 5-HT₄ receptor antagonist [¹¹C]SB207145 for which the in vivo affinity also is investigated.

4.1. Mass effects

If a receptor occupancy below 5% is intended, an upper mass dose limit of 4.5 μg of [¹¹C]SB207145 per 70 kg of body weight can be injected; below 10%, an upper mass dose limit of 9.5 μg for occupancies is required. Interindividual differences in blood–brain barrier uptake, systemic distribution volume, radioligand metabolism, receptor affinity and plasma protein binding are all parameters that can influence the mass dose effects. Nevertheless, the interindividual variations in ID_{50} and mass dose limit determinations (Fig. 2 and Table 1) were relatively moderate.

The occupancy plots generally showed excellent correlations with R^2 between 0.97 and 1.00, and there did not seem to be any major regional differences in occupancy for [¹¹C]SB207145. The peak equilibrium occurs earlier in low-density regions than in high-density regions, which at least theoretically leads to a higher concentration of free and nondisplaceable ligand concentration in the low-density

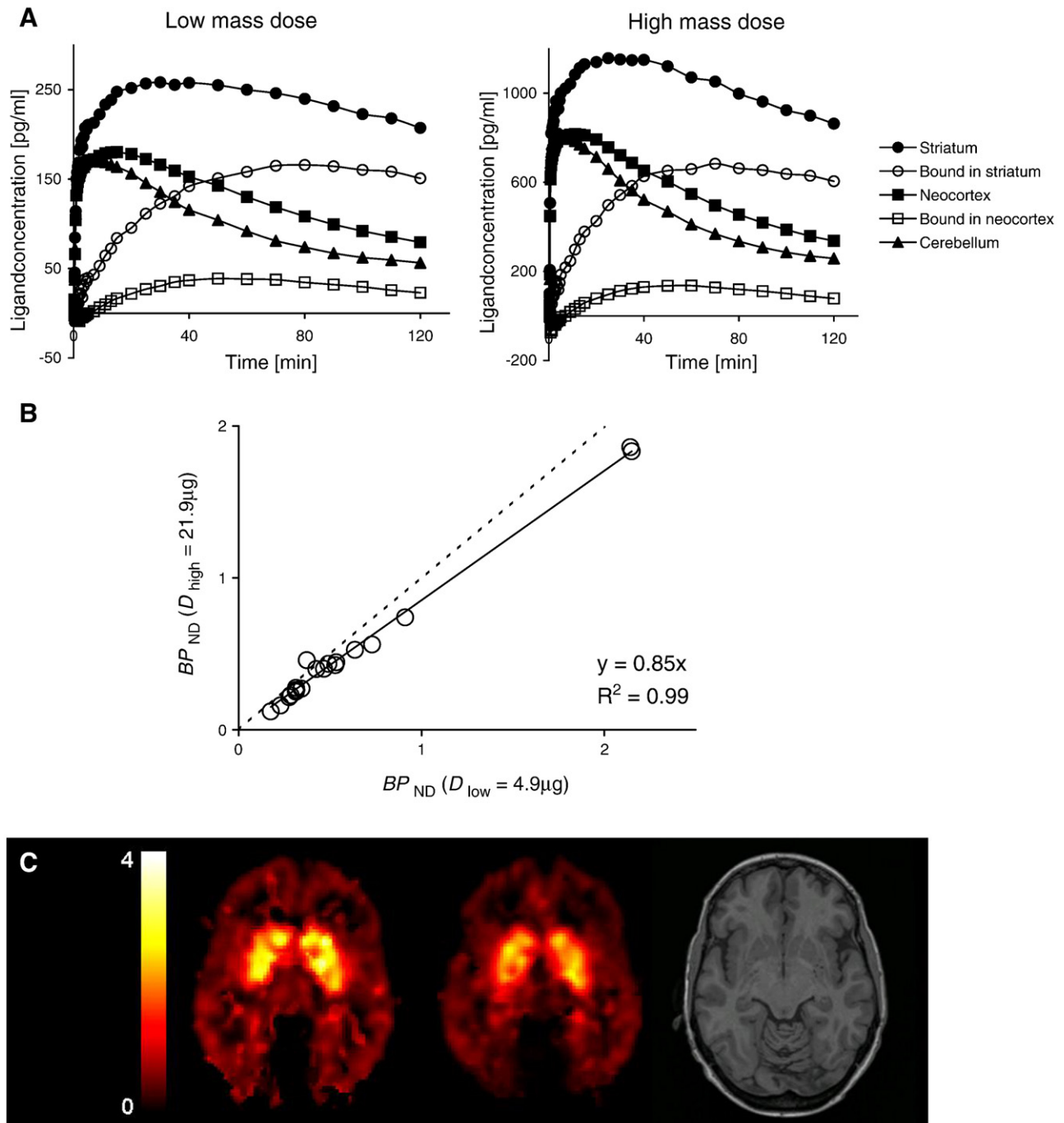


Fig. 1. Examples from one volunteer (1). (A) Regional time concentration curves after intravenous administration of 4.9 μg ligand (left) and 21.9 μg [^{11}C] SB207145 (right). The regional concentration of receptor-bound ligand is the regional concentration subtracted by the cerebellar concentration, which represents the nonspecific and the free ligand. (B) Occupancy plot from the test–retest study for a graphical presentation of the mass effect on BP_{ND} . Each data point represents a single region ($n=19$), and the deviation from line of identity (dotted line) corresponds to the effect of higher mass on the BP_{ND} , i.e., in this example, occupancy is 14%. ID_{50} can be calculated from the slope of the regression line and the upper mass doses limits calculated by Eq. (3). (C) Parametric image of BP_{ND} after injection of 4.9 μg ligand (left) and 21.9 μg ligand (middle) and the corresponding MR image (right).

regions [20]. This would in turn leads to a nonlinearity and intercept with y -axis > 0 in the occupancy plot, which was not observed in this study.

We have previously made a population-based estimate of the upper limit of mass dose (occupancy $< 5\%$) of 1.2 μg [8].

However, our study shows a larger range in mass dose, and test–retest studies with high and low specific activity are more reliable since a population-based study is influenced by interindividual variations in BP_{ND} due to, for example, sex and age effects.

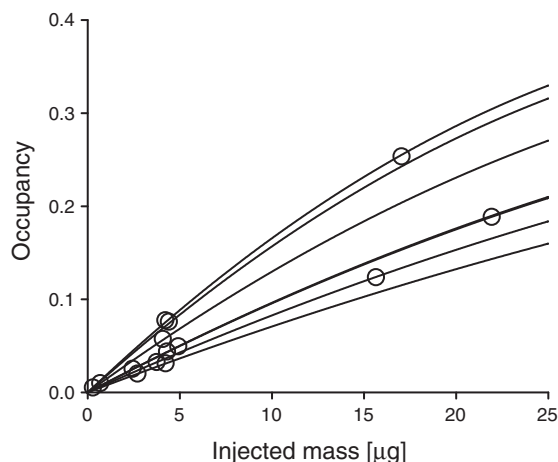


Fig. 2. The lines describe for each individual the association between mass dose and occupancy defined by the ID_{50} . The scans are represented by two data points at the line for each individual. For comparison purposes, the mass doses are normalized to 70 kg of body weight.

The presented method for estimating upper mass dose limits does not require a true baseline scan, and only relatively low occupancies with a limited range are needed. The method can also be used for estimating upper mass dose limits for radiotracers where no suitable reference region is available by using total distribution volumes instead of BP .

Occupancy effects of mass dose should be assessed for all radiotracers, particularly agonists, in order to avoid pharmacological side effects and for the safety of patients and healthy volunteers. Bias from mass dose should also be considered in studies with expected small group differences and in test–retest studies, where carryover effects of mass dose can be a problem, particularly if the affinity is high, and the time interval between scans is short [6]. Mass dose effects are highly relevant in small rodents [21], but may also play a role in human PET studies where variations in bodyweight are expected, for example, in studies of sex differences or diseases associated with altered bodyweight. Furthermore, PET is increasingly used in CNS drug development for investigating the receptor occupancy of drugs [22,23]. In studies of the dose regimen of drugs, it could also be relevant to consider the blocking by the ligand itself, especially when only a small range in receptor occupancy is beneficial, as is the case for the D_2 receptors in antipsychotic treatment [24].

The AUC for cerebellum normalized to injected activity was unaffected by the mass dose, inferring that [^{11}C] SB207145 does not bind specifically in cerebellum, thus supporting the use of cerebellum as a reference region.

We found up to a threefold difference between individuals in the fraction of unmetabolised ligand 55 min postinjection. Metabolic rate can be affected by many factors; however, radiotracer metabolism was not systematically altered by the mass doses given in the present study, i.e., below 22 μg . Only small interindividual variability was found in f_p , and the parameter was

unaffected by the mass dose. The large range in concentration of free parent compound and cerebellar concentration 55 min postinjection is primarily due to differences in injected mass doses. We estimated that the free parent compound accounted for only about 1.5% of the nondisplaceable binding, while the remaining must be nonspecifically bound. However, since equilibrium conditions do not apply 55 min postinjection, we consider that the true free concentration probably constitutes a larger fraction. In any instance, based on our estimates, cerebellum does not mainly represent free compound.

4.2. Affinity

K_D was estimated to an average value of 2.8 nM (range 1.0–4.8) in striatum and neocortex, despite the major effects on the slope of the Scatchard plot of small inaccuracies in the measurements of BP_{ND} . We did not find any difference in the in vivo K_D in high vs. low 5-HT $_4$ receptor density regions; this supports our assumption that free and nondisplaceable ligand was similar in high- and low-binding brain regions at time 80–120 min postinjection and the use of measuring bound at a time interval where the time concentration curves were relatively stable for both regions, rather than time of approximated peak equilibrium, which has been used previously [7]. The relatively low variation is in agreement with the general assumption that interindividual variations in binding potential primarily reflect differences in the available receptor density (B_{avail}), whilst K_D , determined by the structure of the receptor protein and the concentration of the neurotransmitter in question, is expected to be relatively constant between individuals and across brain regions. The estimated in vivo K_D is around sevenfold higher than the in vitro K_D found in the minipig [18]. An around tenfold higher K_D in vivo than in vitro is often found for radioligands [7,25,26] probably because in vivo only a fraction of the radioligand is free and because of non-steady-state conditions.

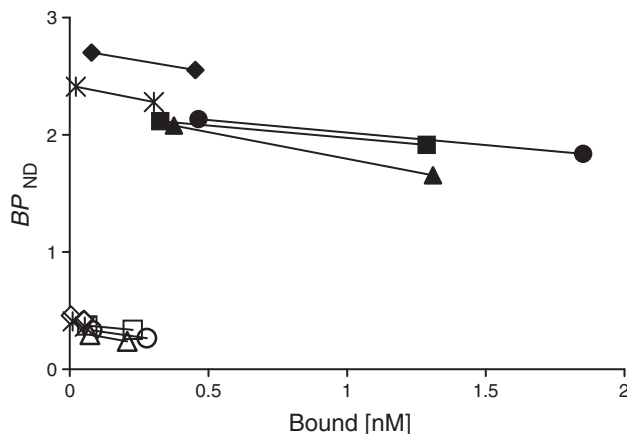


Fig. 3. Scatchard plots of striatum (filled markers) and neocortex (open markers) from test–retest scans with varying mass dose in five subjects. The slope (α) equals $-1/K_D$.

5. Conclusion

This study describes a method for estimating ID_{50} and the upper mass dose limit in validations of new radioligands using test–retest studies with different mass dose. The method can be applied with limited range in occupancy when no true baseline scan is available and despite the absence of a true reference region. Increased mass doses consistently reduced BP_{ND} , as measured with [^{11}C]SB207145, whilst the relative cerebellar uptake was unchanged, thus supporting the use of cerebellum as a reference region in [^{11}C]SB207145 studies. The mass dose required to saturate 50% of receptors (ID_{50}) was $85.4 \pm 30.2 \mu\text{g}$, and the upper mass dose limit (occupancy $<5\%$) was $4.5 \pm 1.6 \mu\text{g}$. The specific activity required for this to be achieved is relatively easily obtained. Within the tested range, radiotracer metabolism and f_p were unaffected by mass dose. In vivo K_D was 2.8 nM (range 1.0–4.8) with no regional differences.

Acknowledgments

Supported by The Lundbeck Foundation, Rigshospitalet, The Toyota Foundation and the Danish Medical Research Council. The John and Birthe Meyer Foundation is gratefully acknowledged for the donation of the Cyclotron and PET scanner.

References

- [1] Innis RB, Cunningham VJ, Delforge J, Fujita M, Gjedde A, Gunn RN, et al. Consensus nomenclature for in vivo imaging of reversibly binding radioligands. *J Cereb Blood Flow Metab* 2007;27:1533–9.
- [2] Lassen NA, Bartenstein PA, Lammertsma AA, Prevett MC, Turton DR, Luthra SK, et al. Benzodiazepine receptor quantification in vivo in humans using [^{11}C]flumazenil and PET: application of the steady-state principle. *J Cereb Blood Flow Metab* 1995;15:152–65.
- [3] Cunningham VJ, Rabiner EA, Slifstein M, Laruelle M, Gunn RN. Measuring drug occupancy in the absence of a reference region: the Lassen plot re-visited. *J Cereb Blood Flow Metab* 2010;30:46–50.
- [4] Mizrahi R, Houle S, Vitcu I, Ng A, Wilson AA. Side effects profile in humans of (11)C-(+)-PHNO, a dopamine D(2/3) agonist ligand for PET. *J Nucl Med* 2010;51:496–7.
- [5] Rabiner EA, Laruelle M. Imaging the D3 receptor in humans in vivo using [^{11}C](+)-PHNO positron emission tomography (PET). *Int J Neuropsychopharmacol* 2010;13:289–90.
- [6] Ashworth S, Rabiner EA, Gunn RN, Plisson C, Wilson AA, Comley RA, et al. Evaluation of 11C-GSK189254 as a novel radioligand for the H3 receptor in humans using PET. *J Nucl Med* 2010;51:1021–9.
- [7] Olsson H, Halldin C, Farde L. Differentiation of extrastriatal dopamine D2 receptor density and affinity in the human brain using PET. *Neuroimage* 2004;22:794–803.
- [8] Marner L, Gillings N, Madsen K, Erritzoe D, Baare WF, Svarer C, et al. Brain imaging of serotonin 4 receptors in humans with [^{11}C]SB207145-PET. *Neuroimage* 2010;50:855–61.
- [9] King MV, Marsden CA, Fone KC. A role for the 5-HT(1A), 5-HT4 and 5-HT6 receptors in learning and memory. *Trends Pharmacol Sci* 2008;29:482–92.
- [10] Lucas G, Rymar VV, Du J, Mnie-Filali O, Bisgaard C, Manta S, et al. Serotonin(4) (5-HT(4)) receptor agonists are putative antidepressants with a rapid onset of action. *Neuron* 2007;55:712–25.
- [11] Cho S, Hu Y. Activation of 5-HT4 receptors inhibits secretion of beta-amyloid peptides and increases neuronal survival. *Exp Neurol* 2007;203:274–8.
- [12] Cachard-Chastel M, Lezoualc'h F, Dewachter I, Delomenie C, Croes S, Devijver H, et al. 5-HT4 receptor agonists increase sAPPalpha levels in the cortex and hippocampus of male C57BL/6j mice. *Br J Pharmacol* 2007;150:883–92.
- [13] Marner L, Gillings N, Comley RA, Baare WF, Rabiner EA, Wilson AA, et al. Kinetic modeling of 11C-SB207145 binding to 5-HT4 receptors in the human brain in vivo. *J Nucl Med* 2009;50:900–8.
- [14] Nelson HE, O'Connell A. Dementia: the estimation of premorbid intelligence levels using the New Adult Reading Test. *Cortex* 1978;14:234–44.
- [15] Derogatis LR. Symptom Checklist-90-R. Administration, scoring, and procedures manual. 3rd edition. Minnesota: National Computer Systems, Minneapolis; 1994.
- [16] Svarer C, Madsen K, Hasselbalch SG, Pinborg LH, Haugbol S, Frokjaer VG, et al. MR-based automatic delineation of volumes of interest in human brain PET images using probability maps. *Neuroimage* 2005;24:969–79.
- [17] Woods RP, Cherry SR, Mazziotta JC. Rapid automated algorithm for aligning and reslicing PET images. *J Comput Assist Tomogr* 1992;16:620–33.
- [18] Kornum BR, Lind NM, Gillings N, Marner L, Andersen F, Knudsen GM. Evaluation of the novel 5-HT4 receptor PET ligand [^{11}C]SB207145 in the Gottingen minipig. *J Cereb Blood Flow Metab* 2009;29:186–96.
- [19] Gillings N. A restricted access material for rapid analysis of [(11)C]-labeled radiopharmaceuticals and their metabolites in plasma. *Nucl Med Biol* 2009;36:961–5.
- [20] Olsson H, Farde L. Potentials and pitfalls using high affinity radioligands in PET and SPET determinations on regional drug induced D2 receptor occupancy — a simulation study based on experimental data. *Neuroimage* 2001;14:936–45.
- [21] Kung MP, Kung HF. Mass effect of injected dose in small rodent imaging by SPECT and PET. *Nucl Med Biol* 2005;32:673–8.
- [22] Cunningham VJ, Gunn RN, Matthews JC. Quantification in positron emission tomography for research in pharmacology and drug development. *Nucl Med Commun* 2004;25:643–6.
- [23] Lee CM, Farde L. Using positron emission tomography to facilitate CNS drug development. *Trends Pharmacol Sci* 2006;27:310–6.
- [24] Howes OD, Egerton A, Allan V, McGuire P, Stokes P, Kapur S. Mechanisms underlying psychosis and antipsychotic treatment response in schizophrenia: insights from PET and SPECT imaging. *Curr Pharm Des* 2009;15:2550–9.
- [25] Farde L, Hall H, Pauli S, Halldin C. Variability in D2-dopamine receptor density and affinity: a PET study with [^{11}C]raclopride in man. *Synapse* 1995;20:200–8.
- [26] Logan J, Volkow ND, Fowler JS, Wang GJ, Fischman MW, Foltin RW, et al. Concentration and occupancy of dopamine transporters in cocaine abusers with [^{11}C]cocaine and PET. *Synapse* 1997;27:347–56.